Comparison of the Resampling Methods for Gridded DEM Downscaling

Nguyen Quang Minh[1*], Nguyen Thi Thu Huong[1], La Phu Hien[1], Duong Thi Tuyet Nhung[1], Nguyen Thi Minh Hong[1], Vu Van Anh[2]

[1] Hanoi University of Mining and Geology, 18 Vien St, Duc Thang, Bac Tuliem, Hanoi

[2] General Department of Remote Sensing, Ministry of Natural Resources and Environment

Abstract. In this paper, a comparison and evaluation of three resampling methods for gridded DEM is implemented. The evaluation was based on the results of bilinear resampling, bi-cubic and Kriging resampling methods for an experiment using both degraded and sampled datasets at 20 m and 60 m spatial resolutions. The evaluation of the algorithms was accomplished comprehensively with visual and quantitative assessments. The visual assessment process was based on direct comparison of the same topographic features in different downscaled images, scatterplots and profiles. The quantitative assessment was based on the most commonly used parameters for DEM accuracy assessment such as root mean square errors (RMSEs), linear regression parameters m and b, and correlation coefficient R. Both visual and quantitative assessment revealed greater accuracy of the Kriging over the other two conventional methods.

1. Introduction

The spatial resolution of a gridded DEM affects both the information content and the accuracy of the data and, potentially, of many other secondary data products [1]. Examples include the well-known effects of spatial resolution on the spatial properties of DEM and other spatial data [2], on slope and aspect [3], watershed boundary delineation and the accuracy of SWAT schemes [4], water run-off models [5], three dimensional modelling of landscapes [6], local slope, plan curvature, drainage area [7], soil survey results and soil moisture [8]. All of the above-mentioned studies showed that DEMs with a finer spatial resolution can produce more informative and more accurate results.

Gridded DEMs with fine spatial resolution and high accuracy can be acquired using remote sensing and airborne LiDAR technology, ground surveying or photogrammetry [9]. Airborne LiDAR enables the acquisition of data with a very high density of 3-dimensional coordinate points and, therefore, production of a DEM with sub-meter spatial resolution. Although being capable of generating a fine spatial resolution DEM, airborne LiDAR technology has some challenges such as the very large amount of data storage required and high computing capacity for data processing. Compared with airborne LiDAR, other methods for fine spatial resolution DEM acquisition such as ground surveying and photogrammetry are more time consuming and labour intensive [10].

Sometimes, it is necessary to resample the raster DEM to a higher resolution using the common algorithms such as nearest neighbour, bilinear and bi-cubic interpolation.

Potentially, these algorithms can downscale the raster DEM data [11]. That means the resolution or the accuracy of raster DEM were slightly improved through resampling using these approaches [12]. Another method for resampling gridded DEM data to a finer resolution Kriging interpolation [13]. Dixon and Earls [14] used the simple nearest neighbour resampling to increase the resolution of DEMs and compare the effects of results to the DEM's products such as stream flow, watershed, delineations, number of sub-basins and slopes. It was showed that the simple resampling of DEM did not increase the accuracy of DEMs greatly, or, the resampling methods did not create new significant information that is not available at the original resolution of DEM [15]. The experiments by Rees [16] and Shi et. al. [12] showed that bilinear, bicubic and Kriging resampling increased the accuracy of DEMs in term of root mean square error (RMSE) with a suitable value of re-sampling ratio *r*. Comparing three resampling methods, Kriging performed better than the other two methods for smooth terrain. However, for terrain with high roughness, the performance of three methods were similar and further assessment of these three methods is necessary [16]. Therefore, in this paper, the evaluation of the algorithms was accomplished comprehensively with visual and quantitative assessments. The visual assessment process was based on direct comparison of the same topographic features in different resampled images, scatterplots and profiles. The quantitative assessment was based on the most commonly used parameters for DEM accuracy assessment such as root mean square errors (RMSEs), linear regression parameters *m* and *b*, and correlation coefficient *R*.

2. Method

To test the three algorithms for resampling, the DEMs with coarser spatial resolution were used as an input to produce DEMs at the same resolution of reference data using the bilinear, bi-cubic resampling, and Kriging interpolation. In the experiment with Kriging interpolation, several Kriging parameters such as semivariogam models, number of samples and range of searching for samples were tested. The most accurate results were selected with Kriging interpolation using exponential variogram model with 8 samples.

The assessment was implemented based on both visual comparison of the resulting DEMs from the three different methods and quantitative evaluation using the parameters which were usually used for DEMs' accuracy assessment such as RMSE [17], coefficient of determination, linear regression parameters, and the elevation profiles [18].

Visual assessment of the results was carried out by several approaches. The first approach is direct visual comparison of the DEM images, especially comparison of the same topographical features in different images. The second approach is to analyse the scatterplots between the elevation values the pixels of reference DEMs and the elevation values of the corresponding pixels of the bilinear and bi-cubic resampled DEMs, and Kriging interpolated DEM. Another approach which was used in many previous research on DEM evaluation is comparing the profiles of the resulted downscaled DEMs [17]. These profiles present the match between the surfaces formed by the reference DEM and the surfaces formed by DEM at coarse spatial resolution, bilinear, bi-cubic and Kriging resampling algorithms and therefore enable the evaluation of the effects of the algorithms on different forms of terrain and topographical features.

The quantitative assessment was implemented mainly based on the RMSEs for whole images and profiles. Together with the RMSEs, the linear regression coefficients such as slope *m*, intercept *b*, and correlation *R* were used to assess the match between the downscaled DEMs from the bilinear and bi-cubic resampling methods, Kriging interpolation and the reference DEMs.

3 Reference and Testing Data

Two types of data were used to evaluate the proposed algorithm. The first type of data was *degraded* coarse DEMs which were calculated from the reference DEMs at fine resolution using nearest neighbour (or averaging method) to make a source of error-free data for algorithm testing. Error-free means the elevation values of pixels in DEM do not contain interpolation and measurement errors. The second type of data is real DEMs which are mostly sampled from point elevation or contour data. Actually, the elevation of a pixel of the DEM represents the elevation of the surface covered by this pixel so it must be the averaged elevation of this surface. The interpolation algorithms are used to estimate this representing elevation from point or contour data so the elevation of a pixel in the real grid DEMs is actually the averaged elevation of all points within the footprint of this pixel with some estimation errors.

The spatial resolution for testing DEM datasets in this paper was selected between 5 m and 60 m and, accordingly, the zoom factor values are 3 or 4. There are two reasons for this selection the spatial resolution. The first reason is because most of currently available sources of grid DEM data are at this range of resolution. The second and more important reason is that the increasing in accuracy of the data at these spatial resolutions is useful for many applications.

The first DEM dataset covered an area of about 3.5 km by 3.5 km and were acquired at Yen Thanh District, Nghe An Province, in North Central Vietnam. The area is located at 18^{o} 58' 57.03" N, 105^{o} 22' 44.87" E, about 45 km from Vinh City. This DEM was produced from topographic maps at the scale of 1:10000. The spatial resolution of the original DEM is 20 m (Fig. 1(a)) and this was degraded to 60 m by averaging the elevation value of 20 m pixels within the footprint of the degraded 60 m (Fig. 1.(b)).

The second dataset was acquired using ground surveying in Lang Son Province of Vietnam. The area of the test field is about 200 m by 200 m in Mai Pha Ward, Lang Son City which is about 150 km from Hanoi. A set of 533 measured elevation points were used with Kriging interpolation to generate a gridded DEM dataset at 5 m spatial resolution for use as a reference, as can be seen in Figure 3(a). The accuracy of reference DEM was assessed based on the ASPRS Accuracy Standard for Digital Geospatial Data [19,20] with a set of 234 validation points. The results of assessment (Table 1) showed that the quality of the reference DEM is slightly better than that of 66.7-cm ASPRS DEM Class and Class VIII of ASPRS 1990 Standards [20] with RMSEz of 48.3 cm and the Appropriate Contourinterval of 1.449-meter. The coarse DEM at 20 m spatial resolution was created using the same interpolation algorithm from the point data (Figure 3(b)). This coarse 20 m DEM was used as input for the algorithms to make 5 m DEM and this result was compared with 5 m DEM reference data.

4. Assessment

Visual comparison showed that the resulting DEMs generated by the bilinear and bi-cubic resampling methods, and Kriging interpolation are visually more similar to the reference DEM than the coarse spatial resolution DEMs for both degraded and sampled datasets. The improvement in visual similarity between the resampled DEMs and reference DEM is seen clearly when comparing between the 20 m DEMs in degraded datasets in Nghe An (Fig. 1) and 5 m and 20 m DEMs resampled datasets with reference DEMs (Fig. 2). While the images of original coarse resolution DEMs and the DEMs by resampling methods, especially the images created by bi-cubic resampling, were blurred with noises and the shapes of terrain features in these images look distorted, the images of Kriging interpolation downscaled DEMs in Fig. 1(e), Fig. 2(e) look less noise and very similar to the reference DEMs in Fig. 1(a), Fig. 2(a). The most clearly improvement of reconstruction of the shapes of terrains can be seen in the marked areas in Fig. 1.

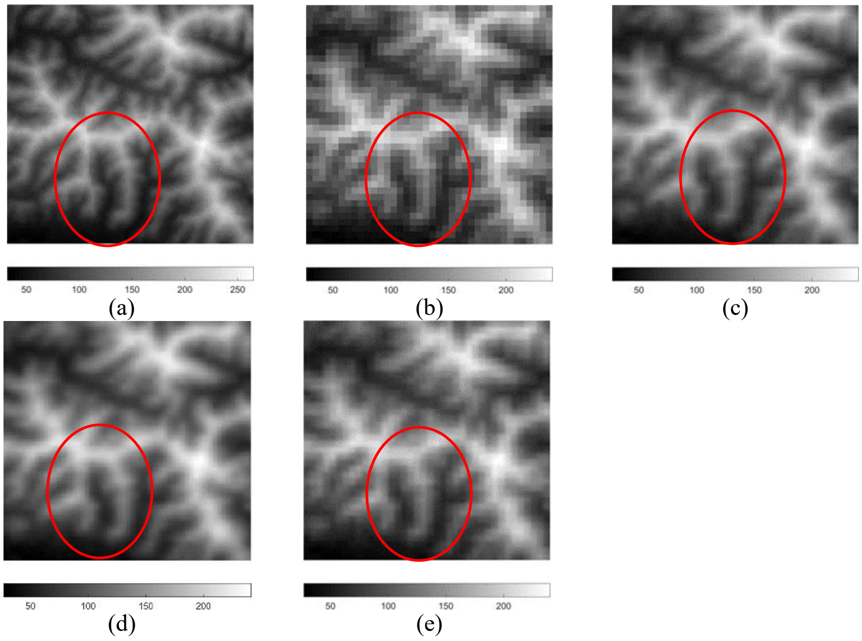

Fig. 1 Downscaling of DEM from 60 m to 20 m spatial resolution. (a) Reference DEM at 20 m resolution; (b) Degraded DEM at 60 m resolution (note: this forms the only input to the algorithms); (c) DEM at 20 m using bilinear resampling; (d) DEM at 20 m resolution using bi-cubic resampling; (e) DEM at 20 m resolution using Kriging interpolation.

The comparison of the surfaces of the resulting DEMs using profiles reveals a clearer advantage of the resampling methods over the original coarse resolution DEM. In

Fig. 3, the elevation profiles of the Kriging interpolated DEMs are closer to the profiles of reference DEMs than those of the bilinear and bi-cubic resampled DEM for both two datasets. This is most clearly seen in the 5 m Lang Son dataset in

Fig. 3(c) (a column profile) and

Fig. 3(d) (a row profile) in places such as tops of hills or bottoms of valleys. In these images, it is possible to observe that the surface formed by the Kriging interpolation DEM are closer to the 5 m reference surface.

The visual comparison of scatterplots in Fig. 4 also showed the better match between the results of the resampling methods and the reference DEM data in comparison with the original coarse DEM. In these scatterplots, the two DEM data are considered to be closer if the data points are located closer to the regression line. That means the slope coefficient *m* is closer to the value of 1 and the intercept coefficient *b* is closer to the value of 0. The scatterplots of the resampling results in Fig. 4 showed a closer match between the reference DEM and the Kriging interpolation DEM data in comparison with the original coarse DEM data, the bilinear and bi-cubic resampling,. The data points in the scatterplots in Fig. 4 showed that it is very close to and (sometime exactly on) the best fit line and the best fit line's coefficients in these scatterplots are closer to the value of 1 and 0.

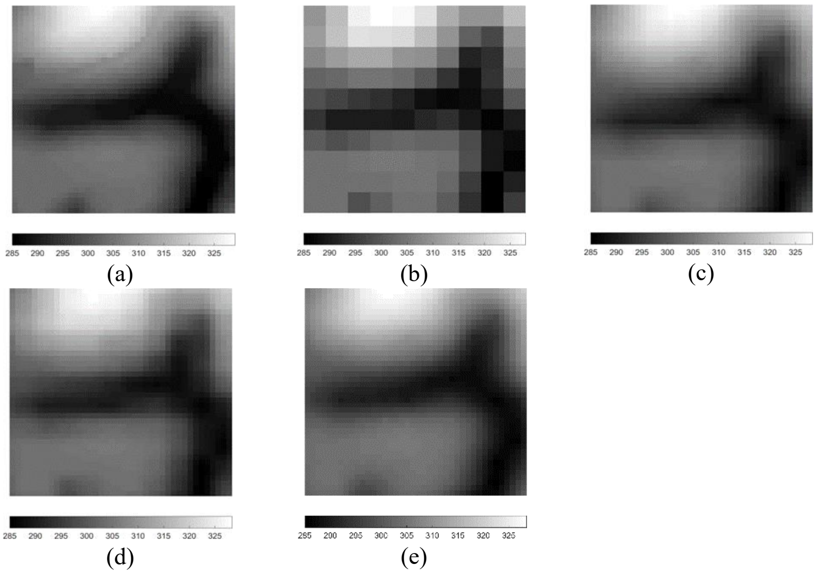

Fig. 2 Downscaling of DEM data from 20 m to 5 m spatial resolution. (a) Reference DEM data at 5 m resolution; (b) Degraded DEM data at 20 m resolution (note: this forms the only input to the algorithms); (c) DEM at 5 m resolution resulted from bilinear resampling; (d) DEM at 5 m resolution resulted from bi-cubic resampling; (e) DEM at 5 m resolution resulted from Kriging interpolation.

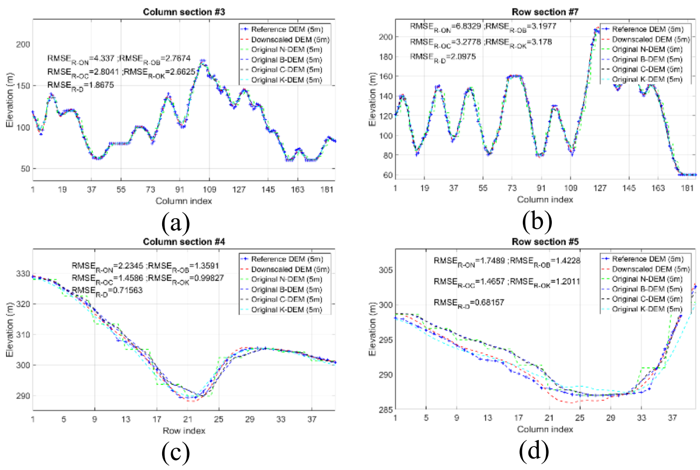

Fig. 3 Comparison of reference surface (reference DEM), original coarse resolution surface (original N-DEM), bilinear (original B-DEM) and bi-cubic (original C-DEM) resampled surfaces based on profiles: (a) a column profile for 20 m degraded dataset in Nghe An; (b) a row profile for 20 m degraded dataset in Nghe An; (c) a column profile for 5 m sampled dataset in Lang Son; (d) a row profile for 5 m sampled Lang Son dataset.

Coinciding with the result of visual observation, quantitative assessment based on the RMSE (Table 1) reveals a greater accuracy for the resampling and Kriging interpolation methods. The RMSEs for the bilinear, bi-cubic resampling and Kriging interpolation methods are 3.3716 m, 3.3716 m and 2.8874 m, respectively. Comparing with the RMSE of the original 60 m data, the RMSE of the resampled DEMs at 20 m reduced significantly for all three methods. The improvement in accuracy for sampled dataset is similar to that of the degraded dataset. The RMSE of 5 m Lang Son data decreased sharply for the resampling algorithms DEM with the values of 1.5139 m for bilinear resampling, 1.6 m for bi-cubic resampling, and 1.2092 m for the Kriging interpolation. These statistics demonstrate that the resampling methods can increase the accuracy of the gridded DEM when it is used to downscale DEM to a finer spatial resolution.

The increase in accuracy in term of RMSE, along with the profiles, demonstrated the effects of the terrain features on the algorithm. For the Nghe An dataset, the increase in accuracy between the original and downscaled DEMs was relatively constant. The similarity of the two DEMs can also be evaluated quantitatively using the linear regression coefficients (m, b) and the correlation coefficient R (Table 2). Comparing two DEMs, if the elevation of a pixel in the reference dataset is x and the elevation of the corresponding pixel in the comparing dataset is y, the expected perfect fit line should be $y = x$ such that $m = 1$ and $b = 0$. Because the value of m may be greater or smaller than 1 and the value of b may be greater or smaller than 0, comparison between different values of m and b to define the closeness of them to 1 and 0, respectively, sometimes it is not easy to evaluate. To make it easier for this evaluation, the sub-parameters such as were calculated. The third parameter for evaluating the fitting of the two datasets is the correlation coefficient R. The correlation coefficient measures the association between two datasets and, thus, captures the distribution of the data points in the scatterplots around the best fit line. The closer value of R^2 to 1, the more data points are located close to the best fit line. A perfect match between two DEM datasets means that all the data points are located on the identity line ($y = x$) and the coefficient of determination $R^2 = 1$. That means the two datasets are exactly the same if the value of m is equal to 1, b is equal to 0 and R^2 is equal to 1, simultaneously.

To evaluate the results of the different methods, linear regression models were fitted to the relation between the reference data and the bilinear and bi-cubic resampled, and Kriging interpolated data. The coefficient values show the better fitting of the Kriging interpolated DEMs with the reference DEMs than those of the original DEMs, bilinear and bi-cubic resampled DEMs. For all four datasets, the values of parameters m, b and R^2 of Kriging interpolated DEMs are much closer to the values of 1, 0, and 1, respectively, than those of the original, bilinear and bi-cubic resampled DEMs. In case of the Lang Son 5 m resampled dataset, the values $|1 - m| = 0.0550$, $|b| = 16.3717$ and $R2 = 0.9884$ for the Kriging interpolated DEM showed greater similarity to the reference DEM than those of the original coarse DEM ($|1 - m| = 0.0310$, $|b| = 9.3306$ and $R2 = 0.9425$), bilinear resampled DEM ($|1 - m| = 0.0399$, $|b| = 12.3782$ and $R2 = 0.9793$), bi-cubic resampled DEM ($|1 - m| = 0.0342$, $|b| = 10.6432$ and $R2 = 0.9763$.

Linear regression coefficients for the 20 m Nghe An degraded dataset showed that the resampled DEM matches very closely to the reference DEM. Surprisingly, the comparison also showed that the original coarse DEM with parameters of $|1-m| = 0.0178$ and $|b| = 2.1147$ is generally more matched (less bias) to the reference DEM than the resampled

Table 1. Root mean squared error for bilinear, bi-cubic, Kriging resampling methods

	Input coarse DEM (m)	**Bilinear (m)**	**Bi-cubic (m)**	**Kriging (m)**	**Accuracy improvement over input DEM (%)**
RMSE for D1 dataset (20 m resolution)					
Overall RMSE	6.9326	3.3026	3.3716	2.8874	71.4
Min CP	3.8029	2.5245	2.5619	2.6330	49.7
Max CP	5.1846	2.9851	3.0731	2.7065	61.1
Min RP	4.5824	2.8843	2.9332	2.8899	57.2
Max RP	6.4972	2.9903	3.0293	2.8799	73.0
RMSE for S1 dataset (5m resolution)					
Overall RMSE	2.4571	1.5139	1.6000	1.2092	65.4
Min CP	1.4960	1.2419	1.2912	0.8727	34.9

Max CP	1.6962	1.1635	1.1821	1.1771	69.8
Min RP	1.7289	1.4081	1.4297	1.4138	35.6
Max RP	1.9510	1.4361	1.5174	1.6807	69.8
RMSE for S2 dataset (30m resolution)					

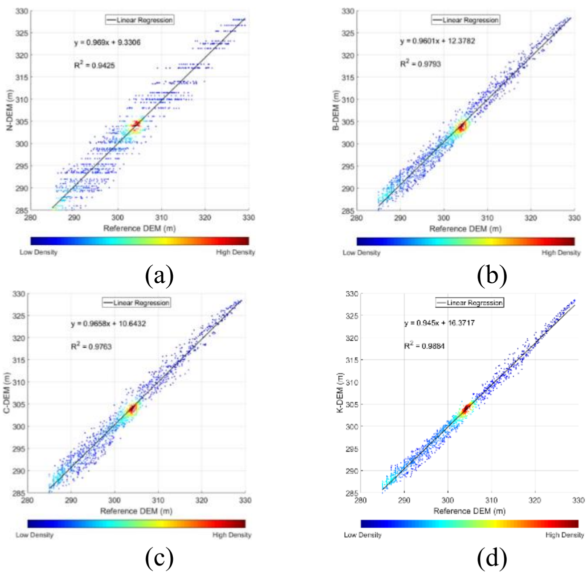

Fig. 4 Scatterplots of the reference fine spatial resolution DEM against the downscaled DEM for the sampled 5 m Lang Son dataset test: (a) the reference DEM and coarse degraded DEM (N-DEM), (b) the reference DEM and the bilinear resampled DEM (B-DEM), (c) the reference DEM and the bi-cubic resampled DEM (C-DEM), (d) the reference DEM and Kriging interpolated DEM (K-DEM).

DEMs with |1 - m| = 0.0235 and |b| = 2.5368, and |1 - m| = 0.0219 and |b| = 2.3680 for bilinear and bi-cubic resampled DEMs, respectively. However, more data points of the bilinear (R^2 = 0.9951) and bi-cubic (R^2 = 0.9948) resampled DEMs are distributed close to the best fit line than those of the original 20 m DEM (R^2 = 0.9770).

Comparing the slope parameter *m* and intercept parameter *b* of the best fit lines of all four datasets, it is clear that all the slope parameters m of the resampled DEMs are smaller than 1 and the intercept parameters *b* are larger than 0. This means that for locally-low places (usually the bottom of valleys) the pixels of the DEM data produced by these methods are likely to be higher than the corresponding pixels in the reference DEM. Conversely, for locally-high places such as the top of hills or mountain ridges, the elevation of the pixels in the resampled DEM data is likely lower than that of the corresponding pixels in the reference image. This is due to the smoothing effect (referred to as conditional bias where highs are under-predicted and lows are over-predicted).

5. Conclusions

A test for resampling algorithms to increase the spatial resolution and accuracy of gridded DEMs was implemented and demonstrated comprehensively using data with different DEM spatial resolutions and characteristics. Tests of the resampling algorithms were implemented on two types of elevation datasets; 20 m DEMs in Nghe An province, Vietnam and a 5 m sampled DEM in Lang Son province. The test results revealed a sharp

increase in accuracy for the Kriging interpolated gridded DEMs in comparison with the original (coarse) gridded DEM, and the bilinear and bi-cubic resampling. Visual assessment revealed the greater similarity of the Kriging interpolated DEMs with the reference DEM than the DEMs generated by bilinear and bi-cubic resampling methods. Quantitative accuracy assessment based on the RMSE revealed an increase in DEM accuracy for the Kriging algorithm over the bilinear and bi-cubic resampling methods. The RMSE of the Kriging interpolated DEMs decreased by approximately 58% and 50%for the 20 m DEMs in Nghe An province and 5 m sampled DEM in Lang son province, respectively.

Table 2. Linear regression coefficients for Nghe An 20 m dataset, and the Lang Son 5 m

Datasets		**Linear Regression Coefficients**		
		m	*b*	R^2
20 m Nghe An dataset	60 m degraded DEM	0.9822	2.1147	0.9770
	20 m bilinear resampled DEM	0.9765	2.5368	0.9951
	20 m bi-cubic resampled DEM	0.9781	2.3680	0.9948
	20 m Kriging interpolated DEM	0.9832	1.8217	0.9962
Lang Son dataset	20 m coarse DEM	0.9690	9.3306	0.9425
	5 m bilinear resampled DEM	0.9601	12.3782	0.9793
	5 m bi-cubic resampled DEM	0.9658	10.6432	0.9763
	5 m Kriging interpolated DEM	0.9450	16.3717	0.9884

Further evaluation was also implemented using linear regression of the original fine spatial resolution DEM against the original, the bilinear and bi-cubic resampled, and Kriging interpolated DEMs, particularly focusing on the coefficients *m*, *b* and *R2*. Analysis of these parameters showed that the Kriging interpolated DEMs was closer to the reference DEMs than the original DEM and those produced using the bilinear and bi-cubic resampling methods.

References

1. S. Saksena and V. Merwade, J. Hydrol. **530**, 180 (2015).
2. Z. Zhao, G. Benoy, T. L. Chow, H. W. Rees, J. L. Daigle, and F. R. Meng, Water Resour. Manag. **24**, 1363 (2010).
3. T. Bolstad, Paul V. & Stowe, ISPRS J. Photogrametric Eng. Remote Sens. **60**, 1327 (1994).
4. K. S. Rawat, G. Krishna, A. Mishra, J. Singh, and S. V. Mishra, J. Appl. Nat. Sci. **6**, (2018).
5. R. F. Vázquez and J. Feyen, J. Hydrol. **334**, 73 (2007).
6. J. M. Schoorl, M. P. W. Sonneveld, and A. Veldkamp, Earth Surf. Process. Landforms (2000).
7. M. P. Smith, A. X. Zhu, J. E. Burt, and C. Stiles, Geoderma **137**, 58 (2006).
8. W. L. Kuo, T. S. Steenhuis, C. E. McCulloch, C. L. Mohler, D. A. Weinstein, S. D. DeGloria, and D. P. Swaney, Water Resour. Res. **35**, 3419 (1999).
9. Q. Guo, W. Li, H. Yu, and O. Alvarez, Photogramm. Eng. Remote Sens. **76**, 701 (2013).
10. X. Liu, Prog. Phys. Geogr. (2008).
11. D. Kidner, M. Dorey, and D. Smith, in *GeoComputation.Org* (1999).
12. W. Shi, B. Wang, and Y. Tian, Math. Geosci. **46**, 445 (2014).
13. C. H. Grohmann and S. S. Steiner, Int. J. Geogr. Inf. Sci. **22**, 895 (2008).
14. B. Dixon and J. Earls, Hydrol. Process. (2009).
15. L. E. Band and I. D. Moore, Hydrol. Process. **9**, 401 (1995).
16. W. G. Rees, Int. J. Remote Sens. **21**, 7 (2000).
17. U. Alganci, B. Besol, and E. Sertel, ISPRS Int. J. Geo-Information **7**, (2018).

18. S. Kienzle, Trans. GIS **8**, 83 (2003).
19. K. Whitehead and C. H. Hugenholtz, Photogramm. Eng. Remote Sens. **81**, 787 (2015).
20. ASPRS, Photogramm. Eng. Remote Sens. **81**, (2015).